Gamma-Ray Bursts, Cosmic-Rays and Neutrinos *

Eli Waxman † ‡ [a]

[a]Dept. of Condensed Matter Physics, Weizmann Institute of Science, Rehovot 76100, Israel

The γ-ray burst (GRB) model for production of ultra-high-energy, $> 10^{19}$ eV, cosmic-rays is based on the hypothesis that GRBs arise from the dissipation of the kinetic energy of relativistic fireballs at cosmological distances. Recent observations of delayed low energy emission, "afterglow," from GRB sources strongly support the validity of this hypothesis. Observations also provide quantitative support for the model. The inferred physical fireball parameters imply that protons may be accelerated to $> 10^{20}$ eV, and the inferred GRB energy generation rate is similar to that required to account for the observed flux of ultra-high-energy cosmic-rays (UHECRs).

Strong suppression of cosmic-ray flux is expected in this model above $10^{19.7}$ eV, due to proton interaction with microwave background photons. Strong deviations from model flux derived under the assumption of uniform source distribution is expected above 10^{20} eV, due to source discreteness and due to inhomogeneities in source distribution. In particular, the flux above $10^{20.5}$ eV is expected to be dominated by few, narrow spectrum sources. While model predictions can not be tested (with high confidence level) using present data, the predicted signatures should be observed with the planned Auger and Telescope-Array UHECR detectors.

A natural consequence of the GRB model of UHECR production is the conversion of a large fraction, $\sim 10\%$, of the fireball energy to accompanying burst of $\sim 10^{14}$eV and $\sim 10^{18}$eV neutrinos. A km^2 neutrino detector would observe several tens of events per year correlated with GRBs, and test for neutrino properties (e.g. flavor oscillations, for which upward moving τ's would be a unique signature, and coupling to gravity) with an accuracy many orders of magnitude better than is currently possible.

1. Introduction

The origin of GRBs, bursts of 0.1 MeV—1 MeV photons lasting for a few seconds, remained unknown for over 20 years, primarily because GRBs were not detected prior to 1997 at wave-bands other than γ-rays (see [1] for review of γ-ray observations). The isotropic distribution of bursts over the sky suggested that GRB sources lie at cosmological distances, and general phenomenological considerations were used to argue that the bursts are produced by the dissipation of the kinetic energy of a relativistic expanding fireball (see [2] for review).

Adopting the cosmological fireball hypothesis, it was shown that the physical conditions in the fireball dissipation region allow Fermi acceleration of protons to energy $> 10^{20}$eV [3,4], and that the average rate at which energy is emitted as γ-rays by GRBs is comparable to the energy generation rate of UHECRs in a model where UHECRs are produced by a cosmological distribution of sources [5]. Based on these two facts, it was suggested that GRBs and UHECRs have a common origin (see [6] for review).

In the last two years, afterglows of GRBs have been discovered in X-ray, optical, and radio wave bands (see [7] for review). Afterglow observations confirmed the cosmological origin of the bursts, through the redshift determination of several GRB host-galaxies (see [8] for an updated list), and confirmed [9] standard model predictions [10] of afterglows that result from the collision of an expanding fireball with its surrounding medium. These observations therefore provide strong support for the GRB model of UHECR production.

In this review, UHECR and neutrino production in GRBs is discussed in the light of recent GRB and UHECR observations. The fireball

*Invited talk presented at TAUP99, the 6th International Workshop on Topics in Astroparticle and Underground Physics (September 1999, Paris, France).

†Incumbent of the Beracha foundation career development chair

‡Work supported in part by BSF Grant 9800343, AEC Grant 38/99 and MINERVA Grant.

model is briefly described in §2.1, and proton acceleration in GRB fireballs is discussed in §2.2. Recent claims, according to which protons can not be accelerated to $> 10^{20}$ eV in the fireball [11], are shown in §2.2 to be erroneous. Implications of recent afterglow observations to high energy particle production are discussed in §3. It is shown that, contrary to some recent claims [12], the GRB energy generation rate implied by afterglow observations is similar to the energy generation rate required to account for the flux of $> 10^{19}$ eV cosmic-rays. Model predictions are shown to be consistent with the observed UHECR spectrum in §4.

Predictions of the GRB model for UHECR production, that can be tested with future UHECR experiments, are discussed in §5. Implications of the detection by the AGASA experiment of multiple high energy events with consistent arrival directions [13] is also discussed in §5. High energy neutrino production in fireballs and its implications for future high energy neutrino detectors are discussed in §6.

2. UHECR from GRB fireballs

2.1. The fireball model

In the fireball model of GRBs [14], a compact source, of linear scale $r_0 \sim 10^7$ cm, produces a wind characterized by an average luminosity $L \sim 10^{52}\mathrm{erg\,s^{-1}}$ and mass loss rate $\dot{M} = L/\eta c^2$. At small radius, the wind bulk Lorentz factor, Γ, grows linearly with radius, until most of the wind energy is converted to kinetic energy and Γ saturates at $\Gamma \sim \eta \sim 300$. Variability of the source on time scale Δt, resulting in fluctuations in the wind bulk Lorentz factor Γ on similar time scale, then leads to internal shocks [15] in the expanding fireball at a radius

$$r_i \approx \Gamma^2 c\Delta t = 3\times 10^{13}\Gamma_{300}^2\Delta t_{10\mathrm{ms}}\ \mathrm{cm}, \qquad (1)$$

where $\Gamma = 300\Gamma_{300}$, $\Delta t = 10\Delta t_{10\mathrm{ms}}$ ms. If the Lorentz factor variability within the wind is significant, internal shocks would reconvert a substantial part of the kinetic energy to internal energy. It is assumed that this energy is then radiated as γ-rays by synchrotron and inverse-Compton emission of shock-accelerated electrons.

In this model, the observed γ-ray variability time, $\sim r_i/\Gamma^2 c \approx \Delta t$, reflects the variability time of the underlying source, and the GRB duration, $T \sim 10$s, reflects the duration over which energy is emitted from the source. A large fraction of bursts detected by BATSE show variability on the shortest resolved time scale, ~ 10 ms [16], and some show variability on shorter time scales, ~ 1 ms [17]. This sets the constraint on underlying source size, $r_0 < c\Delta t \sim 10^7$ cm. The wind must be expanding relativistically, with a Lorentz factor $\Gamma \sim 300$, in order that the fireball pair-production optical depth be small for observed high energy, ~ 100 MeV, GRB photons [18].

The wind Lorentz factor is expected to fluctuate on time scales ranging from the source dynamical time, Δt, to the wind duration T, leading to internal collisions over a range of radii, $r \sim r_i = \Gamma^2 c\Delta t$ to $r \sim \Gamma^2 cT$. Internal shocks are generally expected to be "mildly" relativistic in the fireball rest frame, i.e. characterized by Lorentz factor $\gamma_i - 1 \sim 1$, since adjacent shells within the wind are expected to expand with Lorentz factors which do not differ by more than an order of magnitude.

As the fireball expands, it drives a relativistic shock (blastwave) into the surrounding gas. At early time, the fireball is little affected by this external interaction. At late time, most of the fireball energy is transferred to the surrounding gas, and the flow approaches self-similar expansion. For typical fireball parameters, the transition to self-similar expansion occurs at a radius $r \sim \Gamma^2 cT$. At this radius, mildly relativistic reverse shocks propagate into the fireball ejecta and decelerate it [19]. The reverse shocks disappear on (observed) times scale T, and the flow becomes self-similar at later time, with a single, relativistic decelerating shock propagating into the surrounding medium. Plasma conditions in the reverse shocks are similar to those of internal shocks arising from variability on time scale $\sim T$, since both are mildly relativistic and occur at similar radii. In the discussion that follows we therefore do not discuss the reverse shocks separately from the internal shocks.

The shock driven into the ambient medium continuously heats new gas, and accelerates rel-

ativistic electrons that may produce by synchrotron emission the delayed radiation, "afterglow," observed on time scales of days to months. As the shock-wave decelerates, the emission shifts with time to lower frequency.

2.2. Fermi acceleration in GRBs

In the fireball model, the observed GRB and afterglow radiation is produced by synchrotron emission of shock accelerated electrons. In the region where electrons are accelerated, protons are also expected to be shock accelerated. This is similar to what is thought to occur in supernovae remnant shocks [20]. We consider below proton acceleration in internal (and reverse) fireball shocks. Since the internal shocks are mildly relativistic, we expect results related to particle acceleration in sub-relativistic shocks (see, e.g., [20] for review) to be valid for the present scenario. In particular, the predicted energy distribution of accelerated protons is $dN_p/dE_p \propto E_p^{-2}$.

Two constraints must be satisfied by fireball wind parameters in order to allow proton acceleration to $E_p > 10^{20}$ eV in internal shocks [3]:

$$\xi_B/\xi_e > 0.02\Gamma_{300}^2 E_{p,20}^2 L_{\gamma,52}^{-1}, \tag{2}$$

and

$$\Gamma > 130 E_{20}^{3/4} \Delta t_{10\rm ms}^{-1/4}. \tag{3}$$

Here, $E_p = 10^{20} E_{p,20}$ eV, $L_\gamma = 10^{52} L_{\gamma,52}$erg/s is the γ-ray luminosity, ξ_B is the fraction of the wind energy density which is carried by magnetic field, $4\pi r^2 c\Gamma^2(B^2/8\pi) = \xi_B L$, and ξ_e is the fraction of wind energy carried by shock accelerated electrons. Since the electron synchrotron cooling time is short compared to the wind expansion time, electrons lose their energy radiatively and L is related to the observed γ-ray luminosity by $L_\gamma \approx \xi_e L$. The first condition must be satisfied in order for the proton acceleration time t_a to be smaller than the wind expansion time. The second condition must be satisfied in order for the synchrotron energy loss time of the proton to be larger than t_a.

From Eqs. (2) and (3), we infer that a dissipative ultra-relativistic wind, with luminosity and variability time implied by GRB observations, satisfies the constraints necessary to allow the acceleration of protons to energy $> 10^{20}$ eV, provided that the wind bulk Lorentz factor is large enough, $\Gamma > 100$, and that the magnetic field is close to equipartition with electrons. The former condition, $\Gamma > 100$, is remarkably similar to that inferred based on γ-ray spectra. There is no theory at present that allows a basic principles calculation of the strength of the magnetic field. However, magnetic field close to equipartition, $\xi_B \sim 1$, is required in order to account for the observed γ-ray emission (see also §3).

We have assumed in the discussion so far that the fireball is spherically symmetric. However, since a jet-like fireball behaves as if it were a conical section of a spherical fireball as long as the jet opening angle is larger than Γ^{-1}, our results apply also for a jet-like fireball (we are interested only in processes that occur when the wind is ultra-relativistic, $\Gamma \sim 300$, prior to significant fireball deceleration). For a jet-like wind, L in our equations should be understood as the luminosity the fireball would have carried had it been spherically symmetric.

It has recently been pointed out in [11] that conditions at the *external, highly relativistic* shock driven by the fireball into the ambient gas are not likely to allow proton acceleration to ultra-high energy. Although correct, this observation is irrelevant to the scenario considered here based on [3], since in this scenario protons are accelerated in *internal, mildly relativistic* fireball shocks.

3. Implications of afterglow observations

In addition to providing support to the validity of the qualitative fireball scenario described in §2.1 [7], afterglow observations provide quantitative constraints on fireball model parameters.

The determination of GRB redshifts implies that the characteristic GRB γ-ray luminosity and emitted energy, in the 0.05 to 2 MeV band, are $L_\gamma \sim 10^{52}$erg/s and $E_\gamma \sim 10^{53}$erg respectively (e.g. [8]), an order of magnitude higher than the values assumed prior to afterglow detection (here, and throughout the paper, we assume an open universe, $\Omega = 0.2$, $\Lambda = 0$, and

$H_0 = 75$ km/s Mpc). The increased GRB luminosity scale implies that the constraint (2) on the fireball magnetic field is less stringent than previously assumed.

Due to present technical limitations of the experiments, afterglow radiation is observed in most cases only on time scale $>>$ 10 s. At this stage, radiation is produced by the external shock driven into the surrounding gas, and afterglow observations therefore do not provide direct constraints on the magnetic field energy fraction ξ_B at the internal and reverse shocks, where protons are accelerated to ultra-high energy. In one case, however, that of GRB 990123, reverse shock emission was detected over ~ 10 s time scale [21,22]. For this case, the inferred value of ξ_B [23] is consistent with the constraint (2). Clearly, more observations are required to determine whether this condition is generally satisfied.

The observed GRB redshift distribution implies a GRB rate of $R_{\rm GRB} \sim 10/{\rm Gpc}^3{\rm yr}$ at $z \sim 1$. The present, $z = 0$, rate is less well constrained, since most observed GRBs originate at redshifts $1 \leq z \leq 2.5$ [24]. Present data are consistent with both no evolution of GRB rate with redshift, and with strong evolution (following, e.g., the luminosity density evolution of QSOs or the evolution of star formation rate), in which $R_{\rm GRB}(z=1)/R_{\rm GRB}(z=0) \sim 8$ [24]. The energy observed in γ-rays reflect the fireball energy in accelerated electrons. Afterglow observations imply that accelerated electrons and protons carry similar energy [8]. Thus, the inferred $z = 0$ rate of cosmic-ray production by GRBs is similar to the generation rate of γ-ray energy,

$$E^2(d\dot{n}_{CR}/dE)_{z=0} = 10^{44}\zeta{\rm erg/Mpc}^3{\rm yr}, \qquad (4)$$

where ζ is in the range of ~ 1 to ~ 8. This energy generation rate is remarkably similar to that implied by the observed UHECR flux (see §4).[4]

[4]It has recently been argued [12] that the $z = 0$ GRB γ-ray energy generation rate is much smaller, $\sim 10^{42}{\rm erg/Mpc}^3{\rm yr}$. Most of the discrepancy between this result and our result can be accounted for by noting two errors made in the analysis of ref. [12]: estimating the energy generation rate as the product of the GRB rate and the *median*, rather than *average*, GRB energy, and using (following [25]) the GRB energy observed in the 50 to 300 keV band, where only a small fraction of the 0.05 to 2 MeV γ-ray energy is observed.

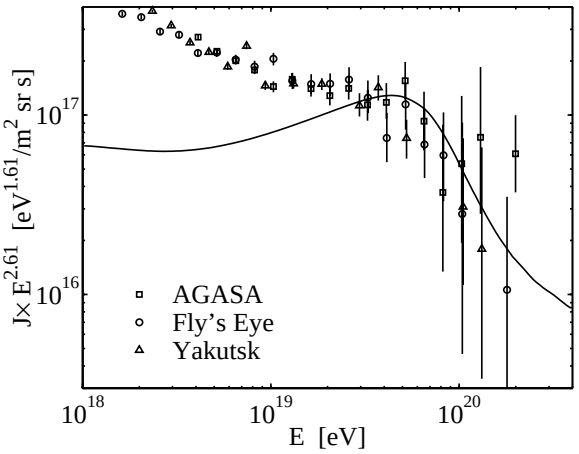

Figure 1. The UHECR flux expected in a cosmological model, where high-energy protons are produced at a rate $(E^2 d\dot{n}_{CR}/dE)_{z=0} = 0.8 \times 10^{44}{\rm erg/Mpc}^3{\rm yr}$ as predicted in the GRB model [Eq. (4)], compared to the Fly's Eye, Yakutsk and AGASA data. 1σ flux error bars are shown. The highest energy points are derived assuming the detected events (1 for Fly's Eye and Yakutsk, 4 for AGASA) represent a uniform flux over the energy range 10^{20} eV–3×10^{20} eV.

4. Comparison with UHECR observations

Fly's Eye [26] and AGASA [27,28] results confirm the flattening of the cosmic-ray spectrum at $\sim 10^{19}$ eV, evidence for which existed in previous experiments with weaker statistics [29]. Fly's Eye data is well fitted in the energy range $10^{17.6}$ eV to $10^{19.6}$ eV by a sum of two power laws: A steeper component, with differential number spectrum $J \propto E^{-3.50}$, dominating at lower energy, and a shallower component, $J \propto E^{-2.61}$, dominating at higher energy, $E > 10^{19}$ eV. The flattening of the spectrum, combined with the lack of anisotropy and the evidence for a change in composition from heavy nuclei at low energy to light nuclei (protons) at high energy [30], suggest that an extra-

Galactic source of protons dominates the flux at high energy $E > 10^{19}$ eV.

In Fig. 1 we compare the UHECR spectrum, reported by the Fly's Eye [26], the Yakutsk [31], and the AGASA [28] experiments, with that predicted by the GRB model. The proton generation rate is assumed to evolve in redshift following QSO luminosity evolution [32]. Note, that the cosmic-ray spectrum at energy $> 10^{19}$ eV is little affected by modifications of the cosmological parameters or of the redshift evolution of cosmic-ray generation rate, since cosmic-rays at this energy originate from distances shorter than several hundred Mpc. The spectrum and flux at $E > 10^{19}$ eV is mainly determined by the present ($z = 0$) generation rate and spectrum. The absolute flux measured at 3×10^{18} eV differs between the various experiments, corresponding to a systematic $\simeq 10\%$ ($\simeq 20\%$) over-estimate of event energies in the AGASA (Yakutsk) experiment compared to the Fly's Eye experiment (see also [27]). In Fig. 1, the Yakutsk energy normalization is used.

The suppression of model flux above $10^{19.7}$ eV is due to energy loss of high energy protons in interaction with the microwave background, i.e. to the "GZK cutoff" [33]. Both Fly's Eye and Yakutsk data show a deficit in the number of events, compared to the number expected based on extrapolation of the $J \propto E^{-2.61}$ power-law fit, consistent with the predicted suppression. The deficit is, however, only at a 2σ confidence level [3]. The AGASA data is consistent with Fly's Eye and Yakutsk results below 10^{20} eV. A discrepancy may be emerging at higher energy, $> 10^{20}$ eV, where the Fly's Eye and Yakutsk experiments detect 1 event each, and the AGASA experiment detects 6 events for similar exposure.

The flux above 10^{20}eV is dominated by sources at distances < 30 Mpc [5] (see §5). Since the distribution of known astrophysical systems (e.g. galaxies, clusters of galaxies) is inhomogeneous on scales of tens of Mpc, significant deviations from model predictions presented in Fig. 1 for a uniform source distribution are expected above 10^{20}eV. It has recently been shown [34] that clustering of cosmic-ray sources leads to a standard deviation, σ, in the expected number, N, of events above 10^{20} eV, given by $\sigma/N = 0.9(d_0/10\mathrm{Mpc})^{0.9}$, where d_0 is the unknown scale length of the source correlation function and $d_0 \sim 10$ Mpc for field galaxies.

An order of magnitude increase in the exposure of UHECR experiments, compared to that available at present, is required to test for the existence of the GZK cutoff [5]. Such exposure would allow this test through an accurate determination of the spectrum in the energy range of $10^{19.7}$ eV to 10^{20} eV, where the effects of source inhomogeneities are expected to be small [5,34]. Moreover, an order of magnitude increase in exposure will also allow to determine the source correlation length d_0, through the detection of anisotropies in the arrival directions of $\sim 10^{19.5}$ eV cosmic-rays over angular scales of $\Theta \sim d_0/30$ Mpc [34].

Finally, we note that preliminary results from the HiRes experiment were presented in this conference [35], reporting 7 events beyond 10^{20} eV for an exposure similar to that of the Fly's Eye. It is difficult to decide how to interpret this result, since the discrepancy between HiRes and Fly's Eye results is present not only above 10^{20} eV but also at lower energy, where Fly's Eye, AGASA and Yakutsk experiments are in agreement: 13 events above 6×10^{19} eV are reported in the preliminary HiRes analysis, while only 5 events at that energy range are reported by the Fly's Eye. We therefore believe that unambiguous conclusions based on the recent HiRes data can only be drawn after a complete analysis of the HiRes data is published.

5. GRB model predictions for planned UHECR experiments

The energy of the most energetic cosmic ray detected by the Fly's Eye experiment is in excess of 2×10^{20}eV, and that of the most energetic AGASA event is $\sim 2 \times 10^{20}$eV. On a cosmological scale, the distance traveled by such energetic particles is small: < 100Mpc (50Mpc) for the AGASA (Fly's Eye) event (e.g., [36]). Thus, the detection of these events over a ~ 5yr period can be reconciled with the rate of nearby GRBs, ~ 1 per 100 yr out to 100Mpc, only if there is a large dispersion, ≥ 100yr, in the arrival time of protons produced in a single burst.

The required dispersion is likely to occur due to the combined effects of deflection by random magnetic fields and energy dispersion of the particles [3]. A proton of energy E propagating over a distance D through a magnetic field of strength B and correlation length λ is deflected by an angle $\theta_s \sim (D/\lambda)^{1/2}\lambda/R_L$, which results in a time delay, compared to propagation along a straight line, $\tau(E,D) \approx \theta_s^2 D/4c \propto B^2\lambda$. The random energy loss UHECRs suffer as they propagate, owing to the production of pions, implies that at any distance from the observer there is some finite spread in the energies of UHECRs that are observed with a given fixed energy. For protons with energies $> 10^{20}$eV the fractional RMS energy spread is of order unity over propagation distances in the range $10 - 100$Mpc (e.g. [36]). Since the time delay is sensitive to the particle energy, this implies that the spread in arrival time of UHECRs with given observed energy is comparable to the average time delay at that energy, $\tau(E,D)$.

The magnetic field required in order to produce a spread $\tau(E = 10^{20}\text{eV}, D = 100\text{Mpc}) > 100$ yr, is well below the current upper bound on the inter-galactic magnetic field, $B\lambda^{1/2} \leq 10^{-9}\text{G Mpc}^{1/2}$ [37], which allows a spread $\tau \sim 10^5$ yr. We discuss below some implications, unique to the GRB model, of time delays induced by magnetic-field deflection.

5.1. The highest energy sources

The rapid increase with energy of the pion production energy loss rate effectively introduces a cutoff distance, $D_c(E)$, beyond which sources do not contribute to the flux above E. The function $D_c(E)$ is shown in Fig. 2. We define a critical energy E_c, for which the average number of sources at $D < D_c(E_c)$ is 1, $\frac{4\pi}{5} R_{GRB} D_c(E_c)^3 \tau\,[E_c, D_c(E_c)] = 1$ [38]. Although E_c depends through τ on the unknown properties of the intergalactic magnetic field, the rapid decrease of $D_c(E)$ with energy near 10^{20}eV implies that E_c is only weakly dependent on the value of $B^2\lambda$. In The GRB model, the product $R_{GRB}\tau(D = 100\text{Mpc}, E = 10^{20}\text{eV})$ is approximately limited to the range $10^{-6}\,\text{Mpc}^{-3}$ to $10^{-3}\,\text{Mpc}^{-3}$ (The lower limit is set by the requirement that at least a few GRB sources be present at $D < 100$ Mpc, and the upper limit by the Faraday rotation bound $B\lambda^{1/2} \leq 10^{-9}\text{G Mpc}^{1/2}$ [37] and $R_{GRB} \leq 10/\,\text{Gpc}^3\text{yr}$). The corresponding range of values of E_c is $10^{20}\text{eV} \leq E_c < 3 \times 10^{20}\text{eV}$.

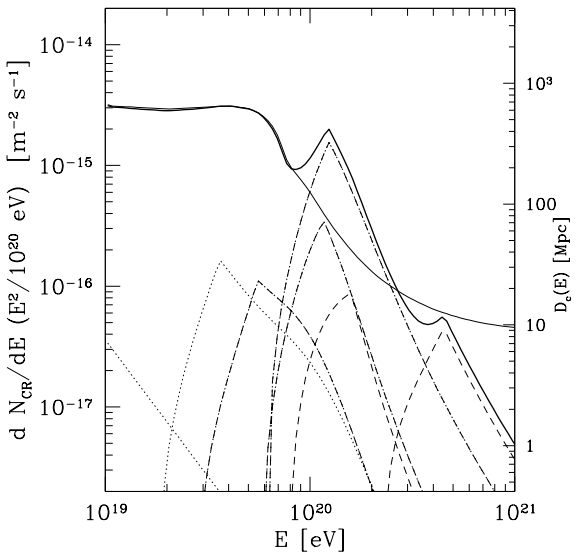

Figure 2. Results of a Monte-Carlo realization of the bursting sources model, with $E_c = 1.4 \times 10^{20}$ eV: Thick solid line- overall spectrum in the realization; Thin solid line- average spectrum, this curve also gives $D_c(E)$; Dotted lines- spectra of brightest sources at different energies.

Fig. 2 presents the flux obtained in one realization of a Monte-Carlo simulation described in ref. [38] of the total number of UHECRs received from GRBs at some fixed time for $E_c = 1.4 \times 10^{20}$ eV. For each realization the distances and times at which cosmological GRBs occurred were randomly drawn. Most of the realizations gave an overall spectrum similar to that presented in Fig. 2 when the brightest source of this realization (dominating at 10^{20}eV) is not included. At $E < E_c$, the number of sources contributing to the flux is very large, and the overall UHECR flux received at any given time is near the average

flux (obtained for spatially and temporally homogeneous UHECR volume emissivity). At $E > E_c$, the flux will generally be much lower than the average, because there will be no burst within a distance $D_c(E)$ having taken place sufficiently recently. There is, however, a significant probability to observe one source with a flux higher than the average. A source similar to the brightest one in Fig. 2 appears $\sim 5\%$ of the time.

At any fixed time a given burst is observed in UHECRs only over a narrow range of energy, because if a burst is currently observed at some energy E then UHECRs of much lower (higher) energy from this burst will arrive (have arrived) mainly in the future (past). For energies above the pion production threshold, $E > 10^{19.7}$eV, the dispersion in arrival times of UHECRs with fixed observed energy is comparable to the average delay at that energy. This implies that the spectral width ΔE of the source at a given time is of order the average observed energy, $\Delta E \sim E$. Thus, bursting UHECR sources should have narrowly peaked energy spectra, and the brightest sources should be different at different energies. For steady state sources, on the other hand, the brightest source at high energies should also be the brightest one at low energies, its fractional contribution to the overall flux decreasing to low energy only as $D_c(E)^{-1}$. A detailed numerical analysis of the time dependent energy spectrum of bursting sources is given in [39].

The AGASA experiment reported the presence of one triplet and three doublets of UHECRs with angular separations (within each multiplet) $\leq 2.5^\circ$, roughly consistent with the measurement error, among a total of 47 UHECRs with $E \geq 4 \times 10^{19}$eV [13]. The probability to have found such multiplets by chance is $\sim 1\%$. Therefore, this observation favors the bursting source model, although more data are needed to confirm it.

Testing the GRB model predictions described above requires an exposure 10 times larger than that of present experiments. Such increase is expected to be provided by the planned Auger [40] and Telescope Array [41] detectors.

5.2. Spectra of Sources at $E < 4 \times 10^{19}$eV

For nearby, $D < 100$ Mpc, sources contributing at $E \leq 4 \times 10^{19}$eV, pion production energy loss is negligible, and particle energy may be considered constant along the propagation path. In this case, the spectral shape of individual sources depends primarily on the magnetic field correlation length [42].

If $\lambda \gg D\theta_s(D,E) \simeq D(D/\lambda)^{1/2}\lambda/R_L$, all UHECRs that arrive at the observer are essentially deflected by the same magnetic field structures, and the absence of random energy loss during propagation implies that all rays with a fixed observed energy would reach the observer with exactly the same direction and time delay. At a fixed time, therefore, the source would appear mono-energetic and point-like (In reality, energy loss due to pair production results in a finite but small spectral and angular width, $\Delta E/E \sim \delta\theta/\theta_s \leq 1\%$ [42]).

If, on the other hand, $\lambda \ll D\theta_s(D,E)$, the deflection of different UHECRs arriving at the observer are essentially independent. Even in the absence of any energy loss there are many paths from the source to the observer for UHECRs of fixed energy E that are emitted from the source at an angle $\theta \leq \theta_s$ relative to the source-observer line of sight. Along each of the paths, UHECRs are deflected by independent magnetic field structures. Thus, the source angular size would be of order θ_s and the spread in arrival times would be comparable to the characteristic delay τ, leading to $\Delta E/E \sim 1$ (The spectral shape of sources is given in analytic form for this case in [42]).

For $D = 30$Mpc and $E \simeq 10^{19}$eV, the $\theta_s D = \lambda$ line divides the allowed region (for the GRB model) in the B–λ plane at $\lambda \sim 1$Mpc. Thus, measuring the spectral width of bright sources would allow to determine if the field correlation length is much larger, much smaller, or comparable to 1Mpc.

6. High energy Neutrinos

6.1. GRB neutrinos, $\sim 10^{14}$ eV

Protons accelerated in the fireball to high energy lose energy through photo-meson interaction with fireball photons. The decay of charged pions

produced in this interaction, $\pi^+ \to \mu^+ + \nu_\mu \to e^+ + \nu_e + \overline{\nu}_\mu + \nu_\mu$, results in the production of high energy neutrinos [43]. The neutrino spectrum is determined by the observed gamma-ray spectrum, which is well described by a broken power-law, $dN_\gamma/dE_\gamma \propto E_\gamma^{-\beta}$ with different values of β at low and high energy [1]. The observed break energy (where β changes) is typically $E_\gamma^b \sim 1$MeV, with $\beta \simeq 1$ at energies below the break and $\beta \simeq 2$ above the break. The interaction of protons accelerated to a power-law distribution, $dN_p/dE_p \propto E_p^{-2}$, with GRB photons results in a broken power law neutrino spectrum, $dN_\nu/dE_\nu \propto E_\nu^{-\beta}$ with $\beta = 1$ for $E_\nu < E_\nu^b$, and $\beta = 2$ for $E_\nu > E_\nu^b$. The neutrino break energy E_ν^b is fixed by the threshold energy of protons for photo-production in interaction with the dominant ~ 1 MeV photons in the GRB [43],

$$E_\nu^b \approx 5 \times 10^{14} \Gamma_{300}^2 (E_\gamma^b/1\mathrm{MeV})^{-1} \mathrm{eV}. \quad (5)$$

The normalization of the flux is determined by the efficiency of pion production. As shown in [43], the fraction of energy lost to pion production by protons producing the neutrino flux above the break, E_ν^b, is essentially independent of energy and is given by

$$f_\pi \approx 0.2 \frac{L_{\gamma,52}}{(E_\gamma^b/1\mathrm{MeV})\Gamma_{300}^4 \Delta t_{10\mathrm{ms}}}. \quad (6)$$

Thus, acceleration of protons to high energy in internal fireball shocks would lead to conversion of a significant fraction of proton energy to high energy neutrinos.

If GRBs are the sources of UHECRS, then using Eq. (6) and the UHECR generation rate given by Eq. (4) with $\zeta \simeq 1$, the expected GRB neutrino flux is [44]

$$E_\nu^2 \Phi_{\nu_x} \approx \quad 1.5 \times 10^{-9} \left(\frac{f_\pi}{0.2}\right) \times \min\{1, E_\nu/E_\nu^b\} \frac{\mathrm{GeV}}{\mathrm{cm^2 s\,sr}}, \quad (7)$$

where ν_x stands for ν_μ, $\bar{\nu}_\mu$ and ν_e.

The neutrino spectrum (7) is modified at high energy, where neutrinos are produced by the decay of muons and pions whose life time exceeds the characteristic time for energy loss due to adiabatic expansion and synchrotron emission [43,45,44]. The synchrotron loss time is determined by the energy density of the magnetic field in the wind rest frame. For the characteristic parameters of a GRB wind, synchrotron losses are the dominant effect, leading to strong suppression of ν flux above $\sim 10^{16}$ eV.

We note, that the results presented above were derived using the "Δ-approximation," i.e. assuming that photo-meson interactions are dominated by the contribution of the Δ-resonance. It has recently been shown [46], that for photon spectra harder than $dN_\gamma/dE_\gamma \propto E_\gamma^{-2}$, the contribution of non-resonant interactions may be important. Since in order to interact with the hard part of the photon spectrum, $E_\gamma < E_\gamma^b$, the proton energy must exceed the energy at which neutrinos of energy E_ν^b are produced, significant modification of the Δ-approximation results is expected only for $E_\nu \gg E_\nu^b$, where the neutrino flux is strongly suppressed by synchrotron losses.

6.2. Afterglow neutrinos, $\sim 10^{18}$ eV

Protons are expected to be accelerated to $> 10^{20}$ eV in both internal shocks due to variability of the underlying source, and in the reverse shocks driven into the fireball ejecta at the initial stage of interaction of the fireball with its surrounding gas, which occurs on time scale $T \sim 10$ s, comparable to the duration of the GRB itself. Optical–UV photons are radiated by electrons accelerated in shocks propagating backward into the ejecta, and may interact with accelerated protons. The interaction of these low energy, 10 eV–1 keV, photons and high energy protons produces a burst of duration $\sim T$ of ultra-high energy, 10^{17}–10^{19} eV, neutrinos [as indicated by Eq. (5)] via photo-meson interactions [47].

Afterglows have been detected in several cases; reverse shock emission has only been identified for GRB 990123 [21]. Both the detections and the non-detections are consistent with shocks occurring with typical model parameters [22], suggesting that reverse shock emission may be common. The predicted neutrino emission depends, however, upon parameters of the surrounding medium that can only be estimated once more observations of the prompt optical afterglow emission are available.

If the density of gas surrounding the fireball is typically $n \sim 1\mathrm{cm}^{-3}$, a value typical to the interstellar medium and consistent with GRB 990123 observations, then the expected neutrino intensity is [47]

$$E_\nu^2 \Phi_{\nu_x} \approx 10^{-10} \left(\frac{E_\nu}{10^{17}\mathrm{eV}} \right)^\beta \frac{\mathrm{GeV}}{\mathrm{cm}^2 \mathrm{s\,sr}}, \qquad (8)$$

where $\beta = 1/2$ for $\epsilon_\nu^{\mathrm{ob.}} > 10^{17}$eV and $\beta = 1$ for $\epsilon_\nu^{\mathrm{ob.}} < 10^{17}$eV. Here too, ν_x stands for ν_μ, $\bar{\nu}_\mu$ and ν_e. The neutrino flux is expected to be strongly suppressed at energy $> 10^{19}$ eV, since protons are not expected to be accelerated to energy $\gg 10^{20}$ eV.

The neutrino flux due to interaction with reverse shock photons may be significantly higher than that given in Eq. (8), if the density of gas surrounding the fireball is significantly higher than the value we have assumed, i.e. if $n \gg 1\mathrm{cm}^{-3}$.

6.3. Implications

The flux of $\sim 10^{14}$ eV neutrinos given in Eq. (7) implies that large area, $\sim 1\mathrm{km}^2$, high-energy neutrino telescopes, which are being constructed to detect cosmologically distant neutrino sources (see [48] for review), would observe several tens of events per year correlated with GRBs. The detection rate of ultra-high energy, $\sim 10^{18}$ eV, afterglow neutrinos implied by Eq. (8) is much lower. The $\sim 10^{18}$ eV neutrino flux depends, however, on parameters of the surrounding medium which can be estimated only once more observations of reverse shock emission are available.

One may look for neutrino events in angular coincidence, on degree scale, and temporal coincidence, on time scale of seconds, with GRBs [43]. Detection of neutrinos from GRBs could be used to test the simultaneity of neutrino and photon arrival to an accuracy of ~ 1 s (~ 1 ms for short bursts), checking the assumption of special relativity that photons and neutrinos have the same limiting speed. These observations would also test the weak equivalence principle, according to which photons and neutrinos should suffer the same time delay as they pass through a gravitational potential. With 1 s accuracy, a burst at 100 Mpc would reveal a fractional difference in limiting speed of 10^{-16}, and a fractional difference in gravitational time delay of order 10^{-6} (considering the Galactic potential alone). Previous applications of these ideas to supernova 1987A (see [49] for review), where simultaneity could be checked only to an accuracy of order several hours, yielded much weaker upper limits: of order 10^{-8} and 10^{-2} for fractional differences in the limiting speed and time delay respectively.

The model discussed above predicts the production of high energy muon and electron neutrinos. However, if the atmospheric neutrino anomaly has the explanation it is usually given, oscillation to ν_τ's with mass ~ 0.1 eV [50], then one should detect equal numbers of ν_μ's and ν_τ's. Up-going τ's, rather than μ's, would be a distinctive signature of such oscillations. Since ν_τ's are not expected to be produced in the fireball, looking for τ's would be an "appearance experiment." To allow flavor change, the difference in squared neutrino masses, Δm^2, should exceed a minimum value proportional to the ratio of source distance and neutrino energy [49]. A burst at 100 Mpc producing 10^{14}eV neutrinos can test for $\Delta m^2 \geq 10^{-16}\mathrm{eV}^2$, 5 orders of magnitude more sensitive than solar neutrinos.

REFERENCES

1. Fishman, G. J. & Meegan, C. A., ARA&A **33**, 415 (1995).
2. Piran, T., in Unsolved Problems In Astrophysics, eds. J. N. Bahcall and J. P. Ostriker, 343-377 (Princeton, 1996).
3. Waxman, E., Phys. Rev. Lett. **75**, 386 (1995).
4. Vietri, M., Ap. J. **453**, 883 (1995).
5. Waxman, E., Ap. J. **452**, L1 (1995).
6. Waxman, E., in Proc. Nobel Symposium *Particle Physics and The Universe* (Haga Slott, Sweden, August 1998), eds. L. Bergstrom, P. Carlson, & C. Fransson (astro-ph/9911395).
7. Mészáros, P., in Proc. *Cosmic Explosions* (Maryland, U.S.A., Oct. 1999), ed. M. Livio (astro-ph/9912474).
8. Freedman, D. L., & Waxman, E., submitted to Ap. J. (astro-ph/9912214).
9. Waxman, E., Ap. J. **485**, L5 (1997); Wijers, R. A. M. J., Rees, M. J. & Mészáros, P., MN-

RAS **288**, L51 (1997).
10. Paczyński, B. & Rhoads, J., Ap. J. **418**, L5 (1993); Katz, J. I., Ap. J. **432**, L107 (1994); Mészáros, P. & Rees, M., Ap. J. **476**, 232 (1997); Vietri, M., Ap. J. **478**, L9 (1997).
11. Gallant, Y. A., & Achterberg, A., MNRAS **305**, L6 (1999).
12. Stecker, F. W. , Submitted to Ap. J. (astro-ph/9911269).
13. Hayashida, N., *et al.* Phys. Rev. Lett. **77**, 1000 (1996); Takeda, M. *et al.*, astro-ph/9902239.
14. Paczyński, B., Ap. J. **308**, L43 (1986); Goodman, J., Ap. J. **308**, L47 (1986).
15. Paczyński, B. & Xu, G., Ap. J. **427**, 708 (1994); Mészáros, P., & Rees, M., MNRAS **269**, 41P (1994).
16. Woods, E. & Loeb, A., Ap. J. **453**, 583 (1995).
17. Bhat, P. N., *et al.*, Nature **359**, 217 (1992).
18. Krolik, J. H. & Pier, E. A., Ap. J. **373**, 277 (1991); Baring, M., Ap. J. **418**, 391 (1993).
19. Mészáros, P., Rees, M., and Papathanassiou, H., Ap. J. **432**, 181 (1994).
20. Blandford, R., & Eichler, D., Phys. Rep. **154**, 1 (1987).
21. Akerlof, C. W. *et al.*, Nature, **398**, 400 (1999).
22. Sari, R. & Piran, T., Ap. J. **517**, L109 (1999); Mészáros, P. & Rees, M., MNRAS **306**, L39 (1999).
23. Waxman, E., & Draine, B. T., Ap. J., in press (astro-ph/9909020).
24. Krumholtz, M., Thorsett, S. E., & Harrison, F. A., Ap. J. **506**, L81 (1998); Hogg, D. W. & Fruchter, A. S., Ap. J. **520**, 54 (1999).
25. Mao, S. & Mo, H. J., A&A **339**, L1 (1998).
26. Bird, D. J., *et al.*, Ap. J. **424**, 491 (1994).
27. Yoshida, S., *et al.*, Astropar. Phys. **3**, 151 (1995).
28. Takeda, M. *et al.*, Phys. Rev. Lett. **81**, 1163 (1998).
29. Watson, A. A., Nucl. Phys. B (Proc. Suppl.) **22B**, 116 (1991).
30. Gaisser, T. K. *et al.*, Phys. Rev. D **47**, 1919 (1993); Dawson, B. R., Meyhandan, R., Simpson, K.M., Astropart. Phys. **9**, 331 (1998).
31. Efimov, N. N. *et al.*, in *Proceedings of the International Symposium on Astrophysical Aspects of the Most Energetic Cosmic-Rays*, edited by M. Nagano and F. Takahara (World Scientific, Singapore, 1991), p. 20.
32. Boyle, B. J. & Terlevich, R. J., MNRAS **293**, L49 (1998).
33. Greisen, K., Phys. Rev. Lett. **16**, 748 (1966); Zatsepin, G. T., & Kuzmin, V. A., JETP lett., **4**, 78 (1966).
34. Waxman, E., & Bahcall, J. N., submitted to Ap. J. (hep-ph/9912326)
35. Matthews, J. N., these proceedings
36. Aharonian, F. A., & Cronin, J. W., Phys. Rev. D **50**, 1892 (1994).
37. Kronberg, P. P., Rep. Prog. Phys. **57**, 325 (1994).
38. Miralda-Escudé, J. & Waxman, E., Ap. J. **462**, L59 (1996).
39. Sigl, G., Lemoine, M. & Olinto, A. V., Phys. Rev. **D56**, 4470 (1997); Lemoine, M., Sigl, G., Olinto, A. V. & Schramm, D. N., Ap. J. **486**, L115 (1997).
40. Cronin, J. W., Nucl. Phys. B (Proc. Suppl.) **28B**, 213 (1992).
41. Teshima, M. *et al.*, Nuc. Phys. **28B** (Proc. Suppl.), 169 (1992).
42. Waxman, E. & Miralda-Escudé, J., Ap. J. **472**, L89 (1996).
43. Waxman, E., & Bahcall, J. N., Phys. Rev. Lett. **78**, 2292 (1997).
44. Waxman, E., & Bahcall, J. N., Phys. Rev. **D59**, 023002 (1999).
45. Rachen, J. P., & Mészáros, P., Phys. Rev. D **58**, 123005 (1998).
46. Muecke, A. *et al.*, PASA **16**, 160 (1999) (astro-ph/9808279).
47. Waxman, E., & Bahcall, J. N., submitted to Ap. J. (hep-ph/9909286)
48. Halzen, F., in Proc. 17th International Workshop on Weak Interactions and Neutrinos (Cape Town, South Africa, January 1999) (astro-ph/9904216).
49. Bahcall, J. N., *Neutrino Astrophysics*, Cambridge University Press (NY 1989).
50. Fukuda, Y., *et al.*, Phys. Lett. **B335**, 237 (1994); Casper, D., *et al.*, Phys. Rev. Lett. **66**, 2561 (1991); Fogli, G. L., & Lisi, E., Phys. Rev. **D52**, 2775 (1995).